

Integrating Ferromagnetism and Ferroelectricity in an Iron Chalcogenide Monolayer: A First-Principle Study

Kaijuan Pang^a, Xiaodong Xu^b, Yadong Wei^b, Tao Ying^a, Weiqi Li^{a,c,*}, Jianqun Yang^b, Xingji Li^b, Yongyuan Jiang^{a,d,e,*}, Guiling Zhang^f, Weiquan Tian^{g,*}

^a School of Physics, Harbin Institute of Technology, Harbin 150001, China

^b School of Material Science and Engineering, Harbin Institute of Technology, Harbin 150001, China

^c State Key Laboratory of Intense Pulsed Radiation Simulation and Effect, Xi'an, 710024, China

^d Collaborative Innovation Center of Extreme Optics, Shanxi University, Taiyuan 030006, China

^e Key Lab of Micro-Optics and Photonic Technology of Heilongjiang Province, Harbin 150001, China

^f School of Materials Science and Chemical Engineering, Harbin University of Science and Technology, Harbin 150080, China

^g School of Chemistry and Chemical Engineering, Chongqing University, Chongqing 401331, China

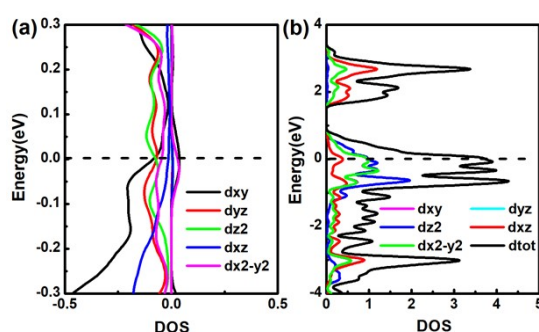


Figure.S1 The density of states (DOS) of FeSSe. (a) spin-polarized (b) non-spin-polarized.

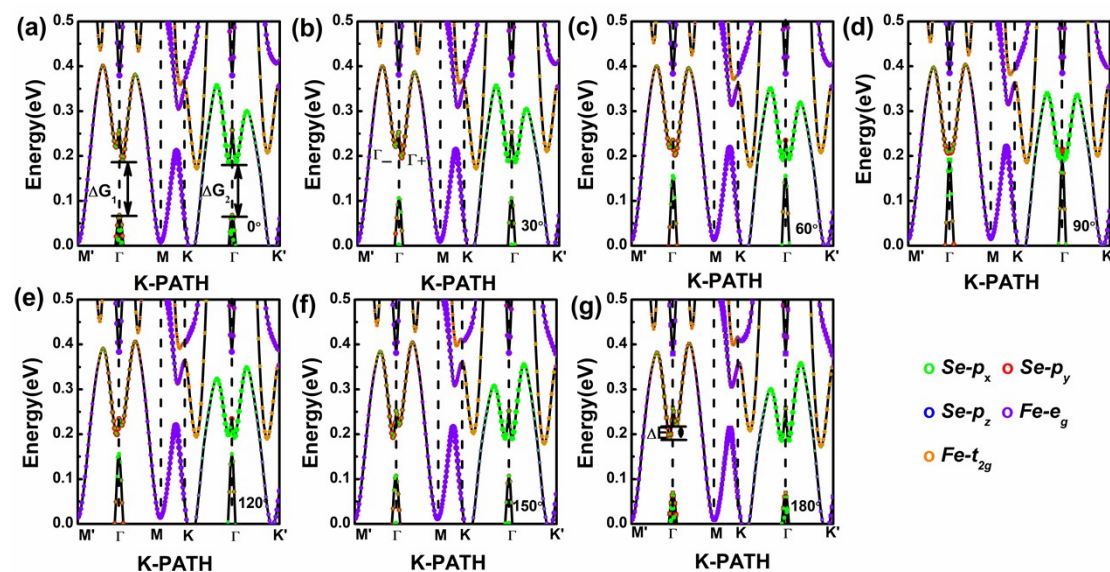


Figure.S2 The orbital-resolved band structure of FeSSe as a function of out-of-plane angle θ with SOC ($\varphi=90^\circ$). The green, red, blue, orange and purple represent $Se-p_x$, $Se-p_y$, $Se-p_z$, $Fe-t_{2g}$ (d_{xy} , d_{yz} , d_{xz}) and $Fe-e_g$ (dx^2-y^2 , dz^2). (a) [0° , 90°]; (b) [30° , 90°]; (c) [60° , 90°]; (d) [90° , 90°]; (e) [120° , 90°]; (f) [150° , 90°]; (g) [180° , 90°].

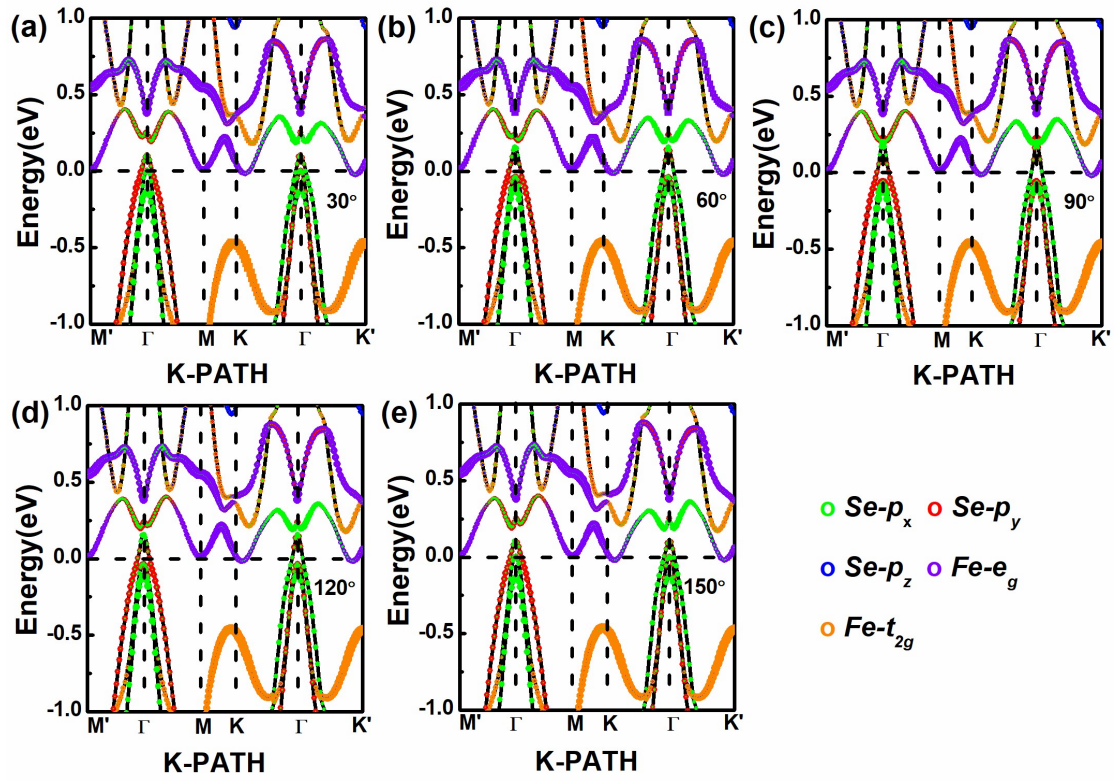


Figure.S3 (a-f) The orbital-resolved band structure of FeSSe as a function of out-of-plane angle θ with SOC ($\varphi=0^\circ$). The green, red, blue, orange and purple represent $Se-p_x$, $Se-p_y$, $Se-p_z$, $Fe-t_{2g}$ (d_{xy} , d_{yz} , d_{xz}) and $Fe-e_g$ (dx^2-y^2 , dz^2). (a) [30° , 0°]; (b) [60° , 0°]; (c) [90° , 0°]; (d) [120° , 0°]; (e) [150° , 0°].

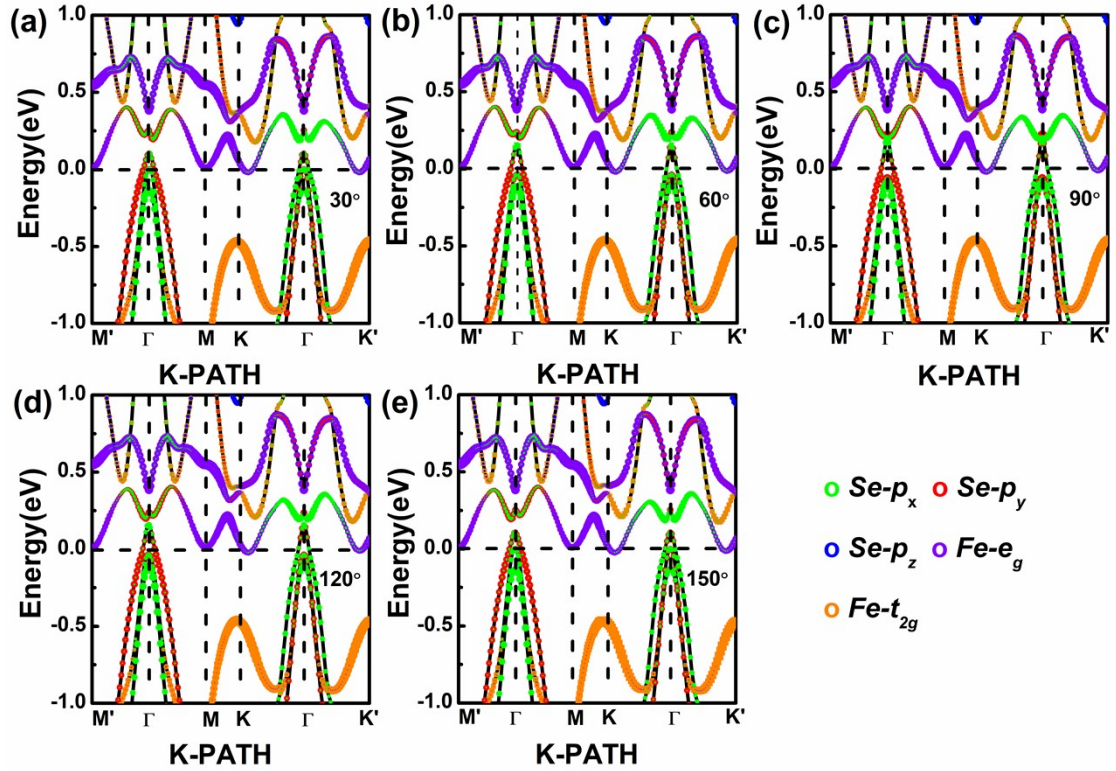


Figure.S4 (a-f) The orbital-resolved band structure of FeSSe as a function of out-of-plane angle θ with SOC ($\varphi=30^\circ$). The green, red, blue, orange and purple represent $Se-p_x$, $Se-p_y$, $Se-p_z$, $Fe-t_{2g}$ (d_{xy} , d_{yz} , d_{xz}) and $Fe-e_g$ (dx^2-y^2 , dz^2). (a)

[30°, 30°]; (b) [60°, 30°]; (c) [90°, 30°]; (d) [120°, 30°]; (e) [150°, 30°].

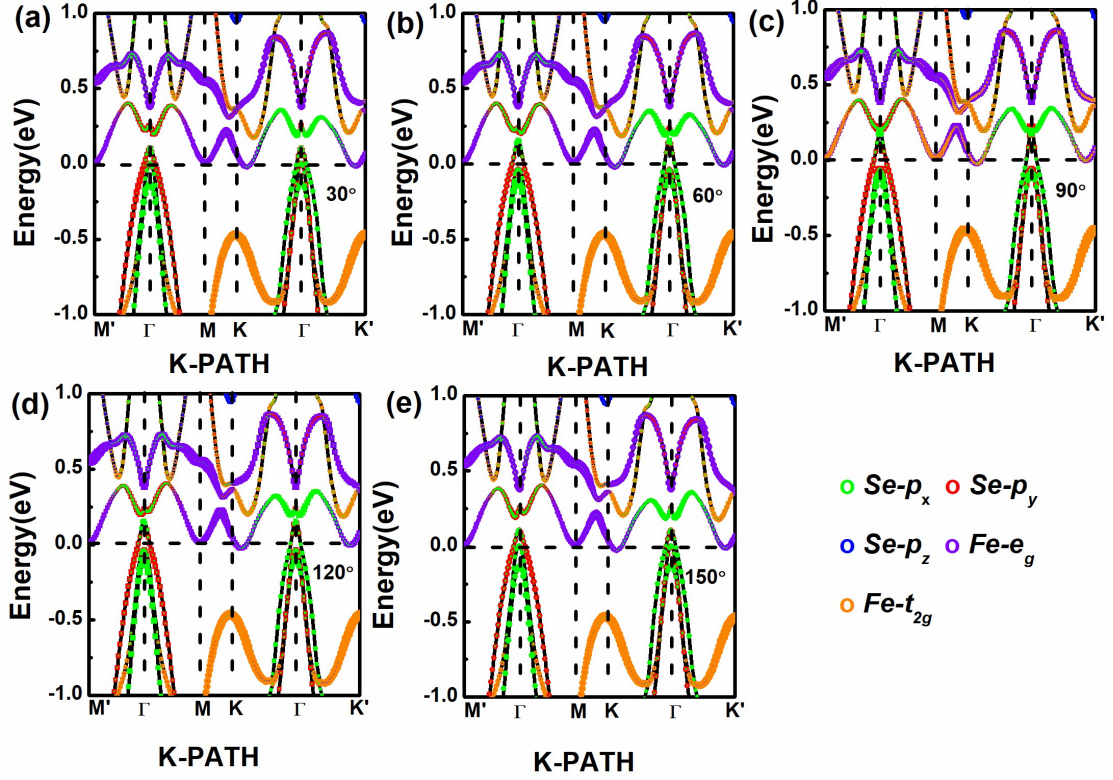


Figure.S5 (a-f) The orbital-resolved band structure of FeSSe as a function of out-of-plane angle θ with SOC ($\varphi=60^\circ$). The green, red, blue, orange and purple represent $\text{Se-}p_x$, $\text{Se-}p_y$, $\text{Se-}p_z$, $\text{Fe-}t_{2g}$ (d_{xy} , d_{yz} , d_{xz}) and $\text{Fe-}e_g$ (dx^2-y^2 , dz^2). (a) [30°, 60°]; (b) [60°, 60°]; (c) [90°, 60°]; (d) [120°, 60°]; (e) [150°, 60°].

Table.S1 The value G_1 , G_2 and ΔE for different $[\theta, \varphi]$.

	[0°,0°]	[30°,0°]	[60°,0°]	[90°,0°]	[120°,0°]	[150°,0°]	[180°,0°]
$\Delta G_1(\text{meV})$	121.31	89.62	46.75	16.82	44.71	86.71	121.36
$\Delta G_2(\text{meV})$	117.38	84.79	37.31	0	36.00	78.78	116.43
$\Delta E(\text{meV})$	29.24	27.66	21.73	0	-14.94	-23.62	-29.00
	[0°,30°]	[30°,30°]	[60°,30°]	[90°,30°]	[120°,30°]	[150°,30°]	[180°,30°]
$\Delta G_1(\text{meV})$	121.31	90.43	47.04	17.20	43.70	85.96	121.36
$\Delta G_2(\text{meV})$	117.38	84.21	36.94	0	37.75	80.17	116.43
$\Delta E(\text{meV})$	29.24	26.69	20.52	0	-16.29	-24.63	-29.00
	[0°,60°]	[30°,60°]	[60°,60°]	[90°,60°]	[120°,60°]	[150°,60°]	[180°,60°]
$\Delta G_1(\text{meV})$	121.31	90.88	47.32	17.60	43.04	85.78	121.36
$\Delta G_2(\text{meV})$	117.38	84.62	36.69	0	40.26	82.07	116.43
$\Delta E(\text{meV})$	29.24	25.41	18.58	0	-18.30	-25.76	-29.00

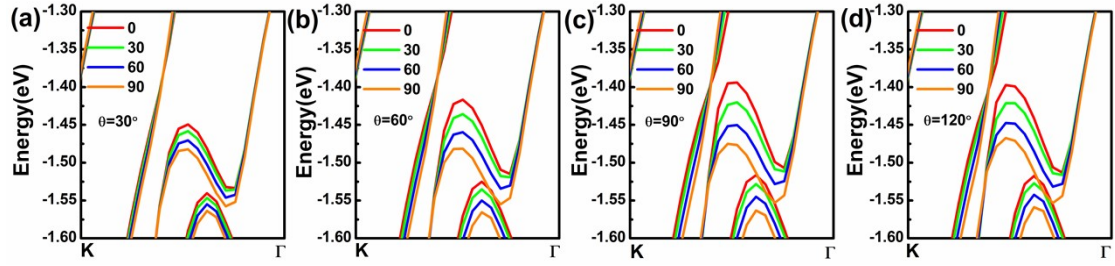


Figure.S6 (a-d) The band structure of FeSSe as a function of in-plane angle with SOC. The red, green, orange and blue represent $\varphi = 0, 30^\circ, 60^\circ, 90^\circ$. (a) $[30^\circ, \varphi]$; (b) $[60^\circ, \varphi]$; (c) $[90^\circ, \varphi]$; (d) $[120^\circ, \varphi]$.

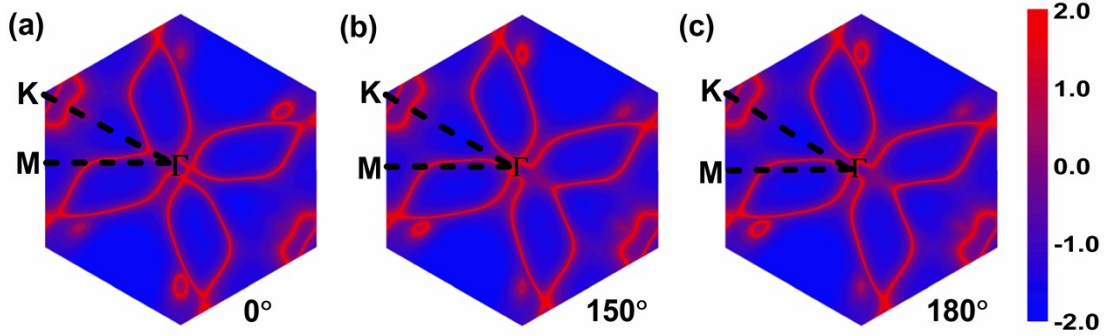


Figure.S7 Magnetization direction-dependent Fermi surfaces of FeSSe. (a) $[0^\circ, 90^\circ]$; (b) $[150^\circ, 90^\circ]$; (c) $[180^\circ, 90^\circ]$.

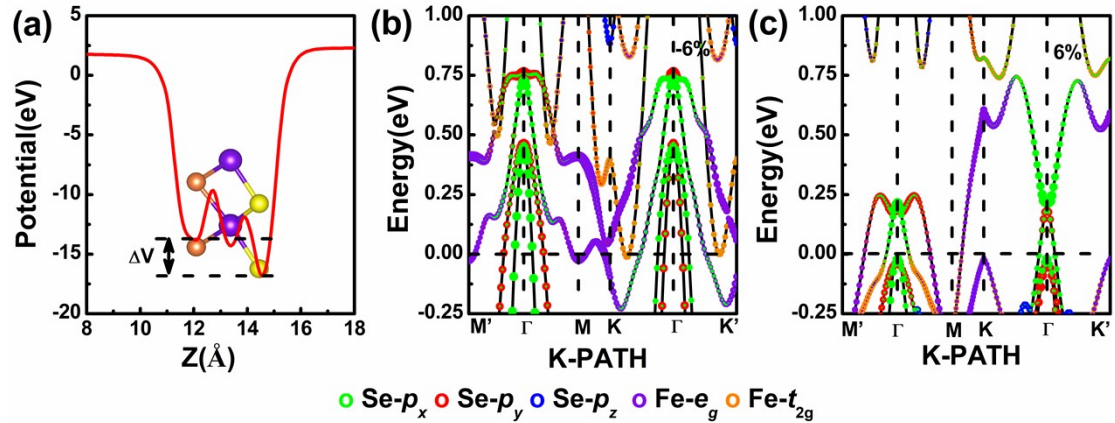


Figure.S8 (a) The average electrostatic potential perpendicular to the surface (ΔV) of FeSSe with FM state without strain. (b-c) The orbital-resolved band structure of FeSSe as a function of biaxial strain with SOC ($\theta=90^\circ, \varphi=90^\circ$). The green, red, blue, orange and purple represent $\text{Se-}p_x, \text{Se-}p_y, \text{Se-}p_z, \text{Fe-}t_{2g} (d_{xy}, d_{yz}, d_{xz})$ and $\text{Fe-}e_g (d_{x^2-y^2}, d_{z^2})$. (b) -6% ; (c) 6% . The color intensity denotes the amplitude of the orbital-resolved character.

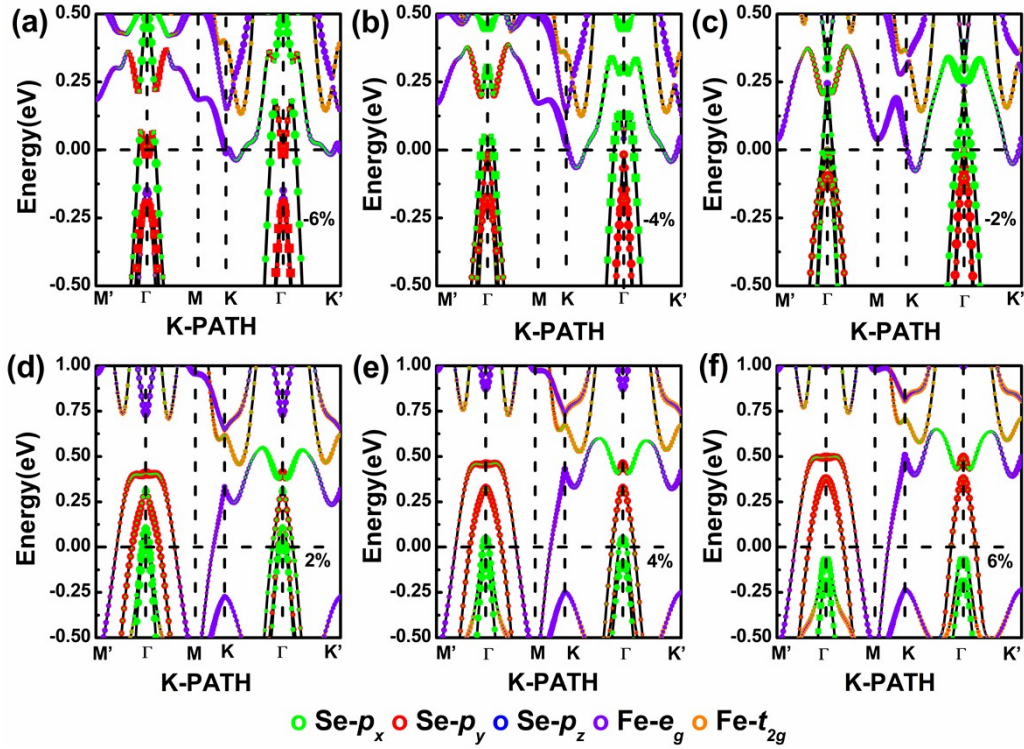


Figure.S9 The orbital-resolved band structure of FeSSe as a function of uni-axially strain with SOC ($\theta=90^\circ$, $\varphi=90^\circ$). The green, red, blue, orange and purple represent Se- p_x , Se- p_y , Se- p_z , Fe- t_{2g} (d_{xy} , d_{yz} , d_{xz}) and Fe- e_g (dx^2-y^2 , dz^2). (a) -6%; (b) -4%; (c) -2%; (d) 2%; (e) 4%; (f) 6%. The color intensity denotes the amplitude of the orbital-resolved character.

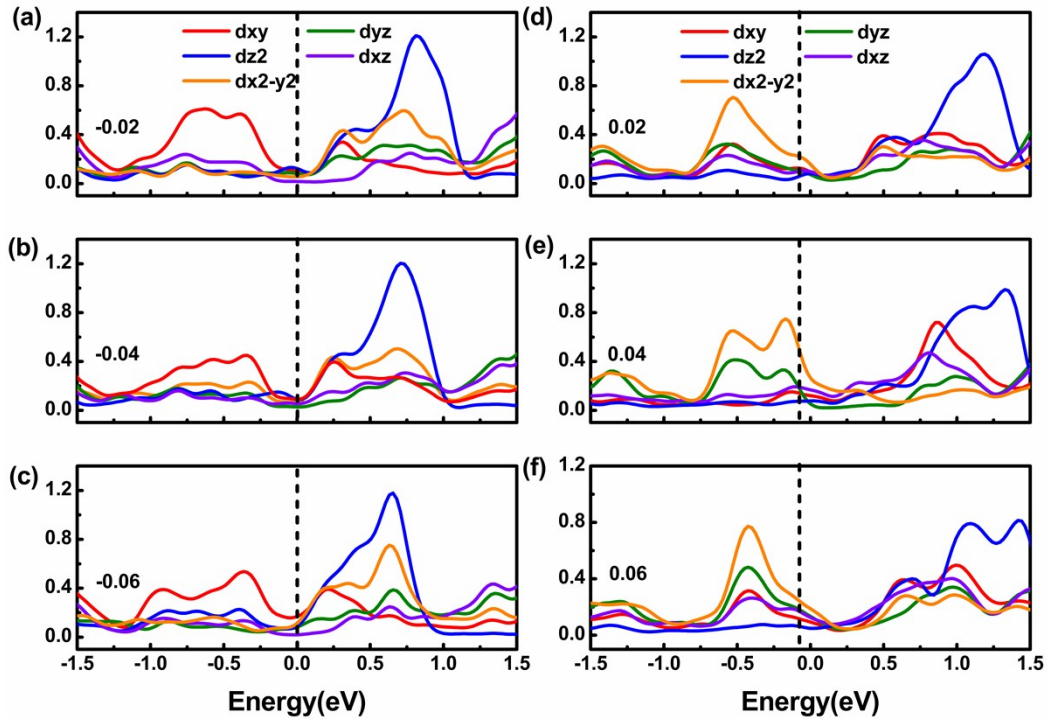


Figure.S10 Project density of state of FeSSe monolayer as a function of biaxial strain in the range of -6% to 6%. (a) -6%; (b) -4%; (c) -2%; (d) 2%; (e) 4%; (f) 6%.

